Spatial measurements near the instability threshold in ultrapure Ge

A. M. Kahn,* D. J. Mar, and R. M. Westervelt
Division of Applied Sciences, Harvard University, Cambridge, Massachusetts 02138
and Department of Physics, Harvard University, Cambridge, Massachusetts 02138
(Received 9 September 1991)

Spatially and temporally resolved measurements are presented near the threshold for a spontaneous current instability in liquid-He-cooled ultrapure Ge. Periodic current oscillations occur above a sharp threshold in applied dc voltage; each cycle is due to the passage of a single space-charge domain through the sample. For sufficiently large applied dc voltage below this threshold, domain formation can be triggered by a small superimposed voltage pulse. As the dc voltage is increased, the triggered domain grows larger and travels farther into the sample. Nearer threshold, current pulses due to single domains spontaneously occur at irregular intervals; as the threshold for spontaneous oscillation is approached, the pulses occur in increasingly larger groups, and the number of pulses per group diverges at the threshold. The statistics of group length and the exponent associated with this divergence agree well with the predictions of Pomeau-Manneville type-III intermittency.

I. INTRODUCTION

A spatial instability occurs in liquid-He-cooled crystals of ultrapure Ge due to impact ionization of shallow acceptors.[1,2] In the post-breakdown regime high-field domains composed of trapped space charge spontaneously nucleate and traverse the sample, producing a periodic current oscillation. Bulk instabilities at low temperatures are also observed in a number of other semiconductors including doped Ge,[3–5] GaAs,[6] InSb,[7] and Si.[8] A classic room-temperature example is the production of high-field domains composed of free space charge in Gunn diodes due to mobility-based negative differential conductivity.[9,10] In cooled ultrapure Ge, high-field domains of trapped space charge are produced by a region of carrier-concentration-based negative differential conductivity resulting from impact ionization of shallow acceptors.[11–13] We have recently presented spatial data describing the motion of space-charge domains in ultrapure Ge for the periodic oscillation.[14]

In this paper we use a movable-capacitive-probe technique and current measurements to examine the transition from spatially homogeneous dc conduction to periodic current oscillations for increasing applied electric field. This transition occurs in a number of steps as the applied field is increased. Well below the threshold applied field E_c for periodic current oscillations the sample is stable, and the transient response to an added pulse is linear. For larger applied fields below the threshold E_c, an added pulse nucleates a space-charge domain which decays as it moves into the sample; with increasing bias the domain grows larger and penetrates farther. At larger applied fields below threshold, domains are spontaneously nucleated and travel into the sample, producing current spikes at irregular intervals. As the threshold E_c for periodic oscillation is approached, the sample displays intermittency in which current spikes cluster into laminar groups of increasing length; at the threshold E_c the laminar length diverges. The statistics of this intermittency agree well with those for a low-dimensional model, Pomeau-Manneville type-III intermittency, even though ours is a spatially extended system.

The organization of this paper is as follows. In Sec. II we describe sample characteristics and experimental techniques. In Sec. III we study the response to a brief upward pulse superimposed on a dc electric field E_b (defined as the applied baseline voltage divided by the sample length) below the threshold for spontaneous current instability. Section IV investigates the onset of the spontaneous instability for increasing dc applied electric field E_{dc} (defined as the applied dc voltage divided by the sample length). Section V shows that the transition to a periodic oscillation occurs via intermittency. Finally, the various thresholds associated with these onset phenomena are summarized in Sec. VI.

II. SAMPLES AND EXPERIMENTAL TECHNIQUES

The sample was cut from a single crystal of undislocated ultrapure Ge with residual shallow acceptor concentration $\sim 1\times 10^{11}$ cm^{-3}, grown by Haller and associates at Lawrence Berkeley Laboratory; the sample characteristics are described in detail in Ref. 14. Samples cut from the same crystal were used for earlier work by Gwinn and Westervelt on the quasiperiodic transition to chaos.[2,15] The sample was cut to size $14.5\times 4.0\times 4.0$ mm^3 and Ohmic contacts were fabricated across opposite 4×4 mm^2 faces by boron ion implantation to produce thin degenerately-doped p^+ layers. These layers act as reservoirs for holes in p-type Ge at liquid-He temperatures. For this geometry the electric field lines lie primarily along the length of the sample. In samples with similar characteristics, we found no evidence for the production of current filaments,[16] which are found in doped material with much higher impurity concentrations.[17] The sample is cooled to 4.2 K in a liquid-He Dewar and is surrounded by cold radiation shields at the same temperature. The measured current-voltage characteristic

for this sample[14] is linear at very low applied fields, but becomes nonlinear and shows a sharp increase in current by many orders of magnitude as impact ionization of the shallow acceptors occurs for an applied dc electric field $E \approx 3.2$ V/cm.

The experimental apparatus used for these measurements is described in detail in Ref. 14. A movable capacitive probe and charge-coupled amplifier are used to measure the time-dependent voltage at a series of locations along the 14.5-mm length of the sample. The data are recorded with a transient recorder and cross plotted to obtain spatial profiles of the sample voltage at successive times. These voltage measurements are calibrated by applying a known oscillating field to the sample in the breakdown regime at a value of dc applied electric field for which the sample response is approximately linear. Spatial derivatives are performed digitally to determine the corresponding sample electric field profiles.

III. TRANSIENT RESPONSE TO A SINGLE PULSE

In this section we study the transient response of the sample when the applied electric field is below the threshold for spontaneous current instability. To investigate the transient response, a brief upward square pulse is added to a baseline dc electric field E_b. The total applied electric field $E_{\text{applied}}(t)$ is given by $E_{\text{applied}}(t) = E_b + E_{\text{pulse}}(t)$, where $E_{\text{pulse}}(t)$ is the time-dependent electric field (defined as the time-dependent voltage divided by the sample length) of the applied pulse. We measure the temporal response of the sample current and the spatially dependent electric field. The temporal response of the sample current is obtained by triggering a transient recorder just prior to the upward pulse and measuring the voltage across a small resistor in series with the sample. Similarly, the electric field at a given location is measured by triggering a transient recorder just prior to the upward pulse and recording the local sample voltage via the movable capacitive probe and a charge-coupled amplifier. The probe is subsequently moved and the process repeated to obtain a spatial profile of the voltage from which we obtain the electric field profile by differentiation. We find that the response of the sample is quite sensitive to the baseline electric field E_b. For a range of baseline fields E_b there is a large nonlinear transient response associated with the nucleation of a high-field domain.[14]

In this paper we examine phenomena very close to the transition to periodic oscillations for increasing dc bias E_{dc}. These phenomena are sensitive to changes in the bias as small as a few mV. During a given experimental run the relevant thresholds in E_{dc} are quite stable relative to this transition and to each other; we find that it is possible to reproducibly measure thresholds to a precision better than 1 mV. Between cooldowns to liquid-He temperature the value of the threshold field E_c at the transition to periodic oscillation varies by a small amount (~ 10 mV), which is greater than the drift within a given run. In order to present a coherent picture using data taken over a period of several months, we present data for dc bias in terms of the normalized bias field ε_{dc}, defined as $\varepsilon_{\text{dc}} = E_{\text{dc}}/E_c$ where E_c is the measured threshold for the transition to periodic current oscillations. Similarly, the response to an applied pulse with baseline field E_b is presented in terms of the normalized baseline field ε_b defined as $\varepsilon_b = E_b/E_c$.

The response of the sample to a small added pulse in applied electric field is shown in Fig. 1 for three increasing values of baseline field. The applied pulse is 40 μs wide and 0.662 V/cm high. Figure 1(a) shows the current response to a pulse with baseline field $\varepsilon_b = 0.8471$, well below the threshold for spontaneous periodic oscillation. The sample response is a sharp rise in the current followed by a return to the dc conduction level, which is slow due to the RC time of the sample. As we show below, the spontaneous instability is characterized by downward current spikes, but in Fig. 1(a) the current does not go below its original level. Spatial measurements confirm that for this value of ε_b the pulse does not nucleate any spatial structures, and the sample can be modeled by a resistor and capacitor in parallel. As the bias is increased, the current response begins to swing below the baseline current for a bias of $\varepsilon_b \approx 0.919$. When the bias is further increased to $\varepsilon_b = 0.9319$, the downward

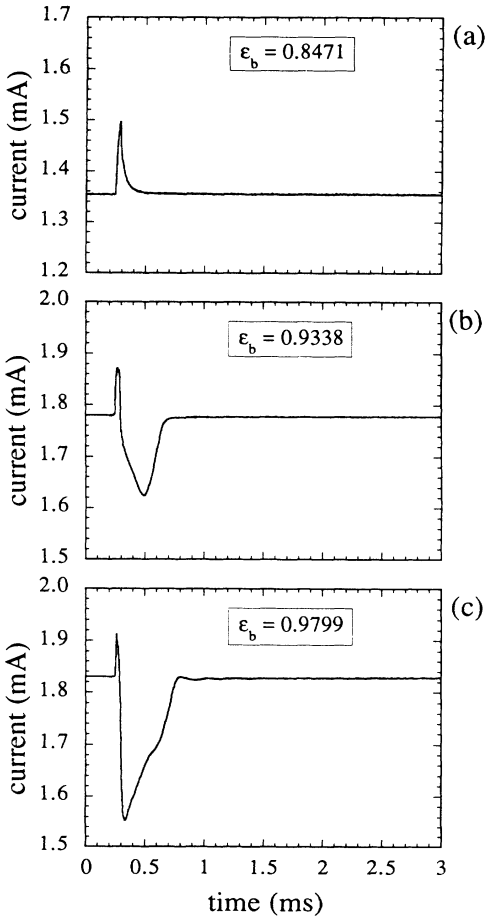

FIG. 1. Total sample current vs time in response to an applied pulse 40 μs wide and 0.662 V/cm high. The pulse begins at $t = 0.25$ ms. The baseline field ε_b indicated on each figure increases from (a)–(c).

swing of the current response suddenly becomes much larger. Figure 1(b) shows the response of the current to a pulse with a baseline $\varepsilon_b = 0.9338$. Following the sharp increase in E_{applied} the current shows a large downward spike which lasts much longer than the applied pulse.

Spatial measurements[14] show that the downward spike corresponds to the nucleation of a high-field domain near the injecting contact. The domain travels into the sample but decays before reaching the receiving contact. As the baseline bias ε_b is further increased, in response to the pulse the downward current spike becomes sharper and deeper, and resembles one period of the periodic current oscillation observed at higher bias fields. These features can be seen in Fig. 1(c), showing the current response with a baseline bias of $\varepsilon_b = 0.9799$.

We have used the movable capacitive probe to map the spatially dependent electric field associated with the response to a pulse for a range of baseline fields. Figure 2 shows the maximum local electric field measured at each position, in response to the same pulse shape as in Fig. 1, for four different values of ε_b. The lowest baseline field corresponds to that used for the time trace in Fig. 1(b) and the highest baseline corresponds to that used for Fig. 1(c). For all of the baseline fields used in Fig. 2, a high-field domain is nucleated near the injecting contact. After an initial growth period, the domain amplitude decays to zero in the bulk of the sample. As the baseline field is increased the initial rate of domain growth increases, the maximum domain amplitude increases, and the domain penetrates farther into the sample.

The maximum electric field taken over all positions and times, in response to the same pulse shape as in Fig. 1 is shown in Fig. 3(a) as a function of baseline field ε_b. As the baseline field is increased by about 5%, the figure shows that the amplitude of the nucleated domain more than doubles. We can define a penetration depth as the location in the sample at which the domain amplitude decays to 10% of its peak value. Figure 3(b) shows the penetration depth of the domain as a function of ε_b. The figure shows that as the threshold for periodic oscillation is approached the penetration depth and the domain amplitude both increase monotonically.

The relation between the current spikes and the measured sample electric field can be understood using a simple model in which the sample is replaced by a voltage source representing the high-field domain, in series with a resistor which represents the remainder of the sample. The sum of the domain voltage and the voltage drop across the sample resistance must equal the applied voltage. Thus a decrease in sample current is associated with a corresponding increase in domain amplitude. A comparison of Fig. 1 with Figs. 2 and 3 shows that the increase in the depth of the current spikes for increasing ε_b is associated with an increase in the amplitude of the nucleated domains. In addition, as ε_b is increased, the increase in the duration of the current spikes is associated with an increase in the penetration depth of the domain.

The spatial data suggest that the criterion for obtaining sustained current oscillation is that a domain penetrates to the receiving contact and nucleates the next domain. Below the onset of spontaneous oscillation, nucleated domains decay before reaching the receiving contact and the sample returns to a spatially homogeneous state. As the baseline field is increased the rate of decay decreases and nucleated domains penetrate farther into the sample. When the applied field is increased into the regime of periodic oscillations, domains penetrate all the way to the receiving contact, and hence succeed in nucleating subsequent domains.[14] Even when domains periodically

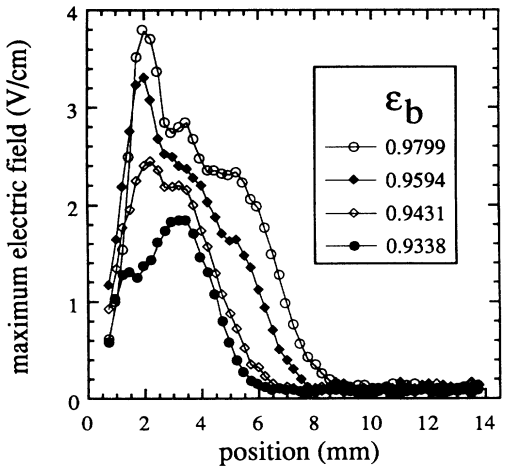

FIG. 2. Maximum electric field at each position in response to a pulse with height and width as in Fig. 1 and baseline field ε_b as indicated in the inset. The lines are guides to the eye.

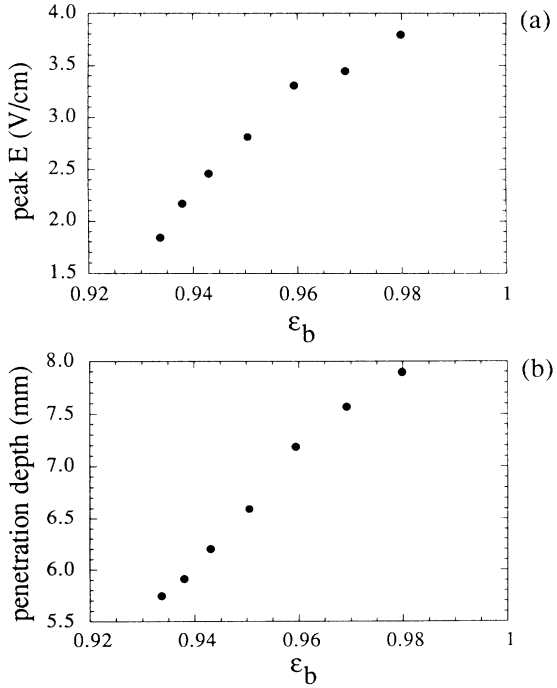

FIG. 3. (a) Peak electric field vs baseline bias field ε_b in response to a pulse with height and width as in Figs. 1 and 2. (b) Penetration depth, defined as the location at which the local electric field decays to 10% of its peak value, vs baseline field ε_b in response to a pulse with height and width as above.

traverse the sample, a decay in domain amplitude is still observed. This suggests that for longer samples the threshold electric field for spontaneous oscillation would be higher.

IV. ONSET OF SPONTANEOUS OSCILLATIONS

This section discusses the onset of spontaneous current oscillations for increasing dc bias ε_{dc}. We observe large downward current spikes occurring at irregular intervals with varying spike heights, where the height of a spike is defined as the difference between the minimum and maximum current during the spike. Spatial measurements presented earlier[14] show that each spike is associated with the nucleation of a high-field domain. As ε_{dc} is increased, the average interval between spikes decreases and at the threshold $\varepsilon_{dc}=1$ we observe a transition to periodic current oscillations.

A spontaneous instability first appears at a dc bias of $\varepsilon_{dc}=0.983$ as a small noisy current oscillation with a fundamental frequency ≈ 6 kHz. For slightly higher bias fields, in addition to the small 6-kHz oscillation, large downward current spikes occur at long irregular intervals. Figure 4 shows five successive time traces of the sample current as ε_{dc} is increased from 0.9873 to 1.001. The time trace in Fig. 4(a) shows the small 6-kHz oscillation and a single current spike occurring at $t=28$ ms, where t is the time coordinate. Following each current spike the amplitude of the 6-kHz oscillation becomes small, and then returns to its original level over the next several ms. As the bias is increased the average interval between groups of spikes decreases and one spike often nucleates another, resulting in increasingly large groups of spikes. Figure 4(b) shows two pairs of spikes occurring 27 ms apart. In Fig. 4(c) with $\varepsilon_{dc}=0.9979$, there are 22 spikes, including a group of eight spikes. In Fig. 4(d), with $\varepsilon_{dc}=0.9992$, longer groups of spikes are observed and the small 6-kHz oscillation returns to its original amplitude almost immediately after each group of spikes. When the bias is increased to $\varepsilon_{dc}=1.000$, the number of spikes in a group diverges and we observe one continuous series of spikes as shown in Fig. 4(e) with $\varepsilon_{dc}=1.001$.

As shown in Fig. 4, the spikes frequently occur in pairs of alternating height, where the height of a spike is defined above. Spatial measurements have shown that the difference in the height of the spikes is associated with both the size of the associated domain and the location in the sample at which the domain is nucleated. The connection between the shape of the spike and the spatially dependent electric field follows from the boundary condition imposed by the fixed voltage bias, as described by the simple model above. Because the integral of the electric field must remain constant, a larger domain results in a proportionately greater decrease in the electric field in the low-field portion of the sample which results in a greater decrease in the current. Longer spikes are associated with larger domains entering the sample at the injecting contact. The shorter spikes are due to proportionately smaller domains. These smaller domains nucleate within the sample, several millimeters from the injecting contact. Hence the domains are in the sample for less time and the shorter spikes are correspondingly briefer in duration.

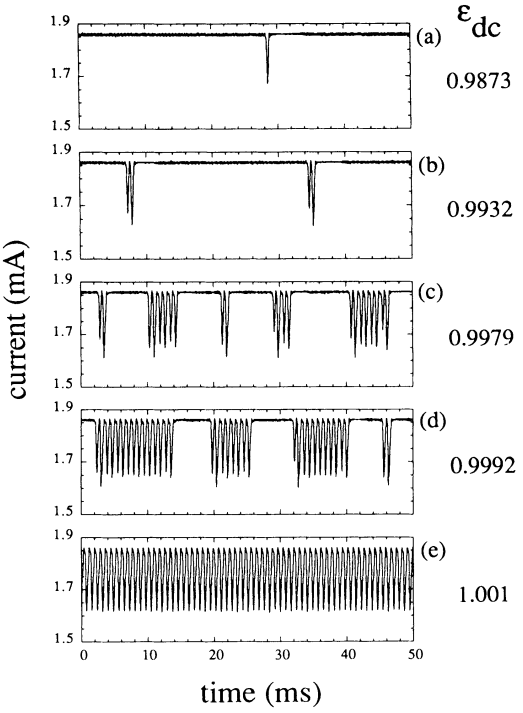

FIG. 4. Time traces of the total sample current for five values of dc bias. The applied field ε_{dc}, indicated at the right, increases from (a)–(e).

V. INTERMITTENCY

In this section we investigate the statistics of the spiking behavior and compare them to the theory of type-III intermittency.[18] Intermittency refers to a phenomenon with intervals of varying lengths of nearly periodic oscillation separated by irregular bursts. The intervals of nearly periodic oscillation are referred to as the laminar regions. Typically, the average laminar length of the laminar regions is a function of an external control parameter. Models of intermittency have been constructed for systems which are well described using a few degrees of freedom. Pomeau and Manneville identified three types of intermittency[19] based upon the way in which a system loses stability. In general, a trajectory in phase space is linearly stable if all the eigenvalues of the Floquet matrix have magnitude smaller than 1. Hence, a transition to intermittency can only occur if one of the eigenvalues leaves the unit circle. Type-III intermittency occurs when the unstable eigenvalue leaves the unit circle in the complex plane at -1 on the real axis.

The theoretical predictions of these models lie in the statistical behavior of intermittent phenomena. Type-III intermittency occurs when a fixed point is marginally unstable so that trajectories starting near the fixed point take a long time to diverge. The time that a trajectory spends near the fixed point corresponds to the laminar regions of oscillation. The amplitude of the oscillations in the laminar region typically alternate in size. After the

trajectory is far away from the fixed point, there is a burst followed by reinjection near the fixed point. The distribution of laminar lengths for type-III intermittency is characterized by a long tail, because the time for destabilization can be arbitrarily long depending on how close to the unstable fixed point the trajectory is reinjected. This is in contrast to type-I intermittency, for which there is a maximum laminar length which cannot be exceeded. Another characteristic of intermittency is the power-law divergence of the average laminar length $\langle l_L \rangle$ as a function of a reduced control parameter:

$$\langle l_L \rangle \propto (A - A_c)^{\alpha} ,$$

where A is the external control parameter and A_c is its value at the transition. In particular, $\alpha = -1$ is predicted for type-III intermittency.

Type-III intermittency has been observed in several experimental systems, including Rayleigh-Bénard convection[20] and conductance oscillations in germanium with a much higher impurity concentration[21] than our samples. In the case of the spontaneous current spiking in our samples, a laminar region corresponds to a group of connected spikes in Fig. 4 and the applied bias is the external control parameter. The number of spikes in a group and the intervals $\tau_{\rm int}$ between spikes are measured from the time series of the sample current. Two spikes are considered to be in the same group if $\tau_{\rm int}$ is less than a threshold value $\tau_{\rm thresh}$. For all data presented here $\tau_{\rm thresh} = 1.2$ ms, approximately 50% longer than the average interval between spikes.

Figure 5(a) shows the bias dependence of the average number of spikes in each laminar region. The inverse of the mean laminar length (in number of spikes) is plotted versus the applied dc bias field. For fields just beyond the onset of the spiking behavior isolated spikes or pairs of spikes predominate. Because the spikes tend to occur in pairs, the average number of spikes shown in Fig. 5(a) is relatively constant for $\varepsilon_{\rm dc} = 0.990$ to $\varepsilon_{\rm dc} = 0.994$, corresponding to a range of bias fields for which the spikes almost always occur in groups of two. For higher bias fields the average laminar length diverges as larger groups of spikes occur more frequently. The fact that the divergence appears as a straight line in the figure suggests that the average laminar length is proportional to $1/(E - E_c)$, where E_c is a critical value of the applied field. We experimentally determine E_c using the power spectrum of the current to determine the onset of periodic oscillations and find that $E_c \approx 6.3$ V/cm. As mentioned above, the exact value of E_c varies by tens of millivolts from run to run. In the notation of this paper, the experimental value of E_c is $\varepsilon_{\rm dc} = 1$. An extrapolation of the straight line divergence in Fig. 5(a) would cross the abscissa at approximately $\varepsilon_{\rm dc} = 1$. Figure 5(b) shows the mean laminar length data of Fig. 5(a) replotted on a log-log scale versus the reduced electric field $(1 - \varepsilon_{\rm dc}) = (E_c - E)/E_c$. As shown, after the step corresponding to the pairs of spikes, the mean laminar length increases as the first power of the reduced electric field. The straight line in the figure is a least-squares fit to the data with mean laminar length greater than 2.1, which

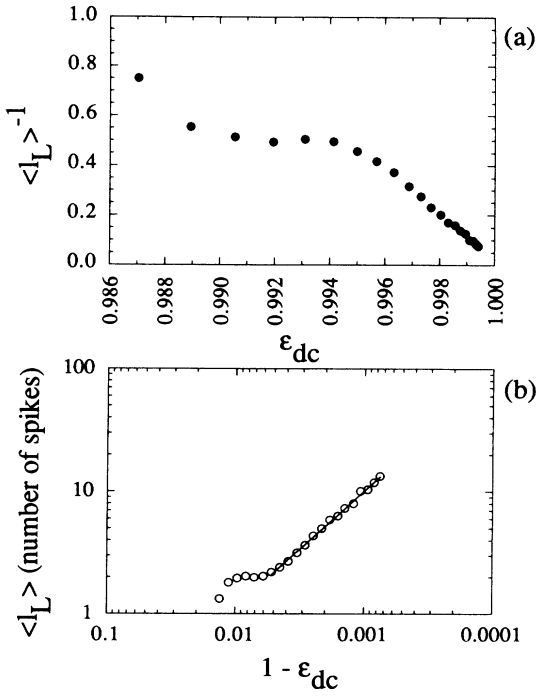

FIG. 5. (a) Inverse of the average laminar length, $\langle l_L \rangle^{-1}$, vs applied electric field $\varepsilon_{\rm dc}$. (b) Log-log graph of the average laminar length $\langle l_L \rangle$ vs the reduced bias field, $1 - \varepsilon_{\rm dc}$. The line is a least-squares fit to the points with mean laminar length greater than 2.1, with an exponent of $\alpha = -0.85$.

gives an exponent $\alpha = -0.85$. This is in good agreement with the exponent $\alpha = -1$ expected for type-III intermittency.

Another measure of intermittent behavior is the distribution $P(l_L)$ of laminar lengths observed for fixed control parameters. As discussed above, type-III intermittency is characterized by a length distribution with a long tail. This tail has the approximate form $P(l_L) \propto \exp(-2\beta l_L)$ where $\beta = 1 - \varepsilon_{\rm dc}$ is the reduced control parameter.[18] Figure 6 shows the distribution of laminar lengths observed for a 2-sec time series with fixed dc bias $\varepsilon_{\rm dc} = 0.9988$

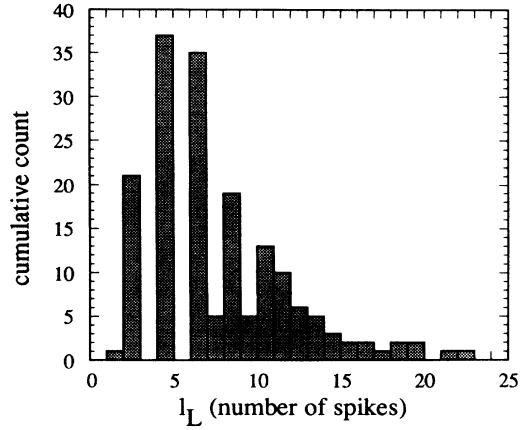

FIG. 6. Histogram of the distribution of laminar lengths l_L observed for fixed dc bias field $\varepsilon_{dc} = 0.9988$.

which results in a mean laminar length equal to 7.3. The alternation between peaks in Fig. 6 is due to the fact that the spikes tend to occur in pairs, resulting in many more even-numbered laminar lengths, especially for shorter lengths. The long tail in the distribution is a characteristic of type-III intermittency.

The power-law divergence of the laminar length, the laminar-length critical exponent close to unity, the long tail in the histogram of laminar lengths, and the alternation in spike amplitudes are all characteristic of type-III intermittency. It is interesting that the spiking behavior near onset is well described by the model of type-III intermittency, because this is often associated with low-dimensional dynamics and our system is spatially extended with potentially many degrees of freedom. The nonlaminar intervals in type-III intermittency correspond then to intervals in which no domain is present in the sample. As shown in Fig. 4, the current displays excess noise between spikes, which one could associate with chaotic bursts in a low-dimensional model of type-III intermittency. However, in the absence of domains it is not clear whether a simple low-dimensional model can describe this spatially extended system.

VI. SUMMARY AND CONCLUSIONS

As the applied electric field is increased a number of threshold values have been identified. These are summarized in Table I, where ε refers to the relevant normalized electric field, ε_b or ε_{dc}. The first important threshold in the system is the impurity breakdown field, $\varepsilon=0.516$. As the field is increased we are first able to nucleate high-field domains using an applied pulse with a baseline field $\varepsilon=0.927$. A spontaneous instability is first observed as a noisy 6-kHz oscillation for $\varepsilon=0.983$. When the bias is increased to $\varepsilon=0.984$ large downward current spikes associated with moving space-charge domains are observed. Finally, at $\varepsilon=1.000$ a large periodic current oscillation is observed when each domain traversing the sample succeeds in nucleating a subsequent domain.

TABLE I. Summary of threshold values for increasing electric field.

Threshold field (V/cm)	ε	Transition
3.2	0.516	Impurity breakdown
5.80	0.927	Able to nucleate domains with an applied pulse
6.18	0.983	Onset of noisy 6-kHz oscillation
6.19	0.984	Onset of spiking
6.29	1.000	Onset of periodic oscillation (E_c)

In conclusion, we have presented spatial and temporal measurements of the onset of oscillations due to moving space-charge domains in ultrapure Ge. For bias fields below the onset of the oscillation, a large downward current spike due to the nucleation of a high-field domain is observed in response to a brief pulse in the applied electric field. As the baseline bias field is increased the current response becomes larger and the nucleated domain penetrates farther into the sample. For dc bias just below the threshold for spontaneous periodic current oscillations, single pulses are intermittently nucleated either singly or in bursts. The statistics of this intermittent phenomenon agree well with those of type-III intermittency even though our physical system is spatially extended with potentially many degrees of freedom.

ACKNOWLEDGMENTS

We thank L. L. Bonilla, S. H. Strogatz, and S. W. Teitsworth for helpful discussions. One of us (D.J.M.) acknowledges financial support from AT&T Bell Laboratories. This work was supported in part by the Office of Naval Research under Grant No. N00014-89-J-1592.

*Present address: Department of Physics, University of California, Santa Barbara, CA 93106.

[1]S. W. Teitsworth, R. M. Westervelt, and E. E. Haller, Phys. Rev. Lett. **51**, 825 (1983).
[2]E. G. Gwinn and R. M. Westervelt, Phys. Rev. Lett. **57**, 1060 (1986), **59**, 247(E) (1987).
[3]B. K. Ridley and R. G. Pratt, J. Phys. Chem. Solids **26**, 21 (1965).
[4]J. Peinke, A. Mühlbach, R. P. Huebener, and J. Parisi, Phys. Lett. **108A**, 407 (1985).
[5]G. A. Held, C. Jeffries, and E. E. Haller, Phys. Rev. Lett. **52**, 1037 (1984).
[6]K. Aoki and K. Yamamoto, Phys. Lett. **98A**, 72 (1983).
[7]D. G. Seiler, C. L. Littler, R. J. Justice, and P. W. Milonni, Phys. Lett. **108A**, 462 (1985).
[8]K. Yamada, N. Takara, H. Imada, N. Miura, and C. Hamiguchi, Solid State Electron. **31**, 809 (1988).
[9]J. B. Gunn, Solid State Commun. **1**, 88 (1963).
[10]Reviewed in P. N. Butcher, Rep. Prog. Phys. **30**, 97 (1967).
[11]S. W. Teitsworth, Appl. Phys. A **48**, 127 (1989).
[12]V. V. Mitin, Appl. Phys. A **39**, 123 (1986).
[13]L. L. Bonilla and S. W. Teitsworth, Physica D **50**, 545 (1991).
[14]A. M. Kahn, D. J. Mar, and R. M. Westervelt, Phys. Rev. B **43**, 9740 (1991).
[15]E. G. Gwinn and R. M. Westervelt, Phys. Rev. Lett. **59**, 157 (1987).
[16]A. M. Kahn, D. J. Mar, and R. M. Westervelt, Solid State Electron. **32**, 1143 (1989).
[17]J. Peinke, J. Parisi, B. Röricht, K. M. Mayer, U. Rau, W. Clauss, R. P. Huebener, G. Jungwirt, and W. Prettl, Appl. Phys. A **48**, 155 (1989), and references therein.
[18]See, for example, H. G. Schuster, *Deterministic Chaos,* 2nd ed. (VCH, Weinheim, Germany, 1989).
[19]Y. Pomeau and P. Manneville, Commun. Math. Phys. **74**, 189 (1980).
[20]M. Dubois, M. A. Rubio, and P. Berge, Phys. Rev. Lett. **51**, 1446 (1983).
[21]R. Richter, J. Peinke, W. Clauss, U. Rau, and J. Parisi, Europhys. Lett. **14**, 1 (1991).

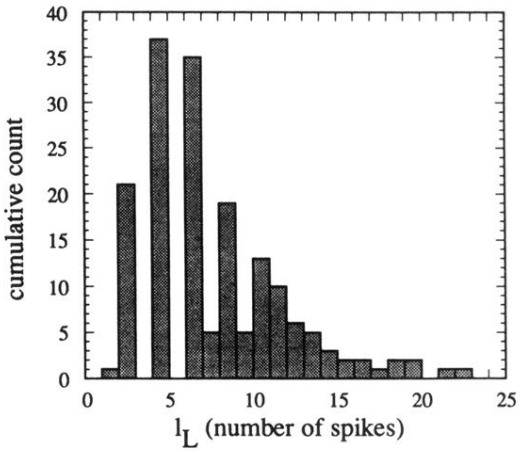

FIG. 6. Histogram of the distribution of laminar lengths l_L observed for fixed dc bias field $\varepsilon_{dc} = 0.9988$.